Electronic Supplementary Information

Experimental section

Materials: Commercially pure Ag foil (99.99%, 0.25 mm in thickness), acetone, ethanol, sodium bromide (NaBr) and ethylene glycol (EG) were purchased from Tianjin Chemical Reagent Corporation. All chemical regents were used as received without further purification. Ultrapure water we used during the experiment process was purified through a Millipore system.

Characterization: Powder XRD data were acquired on a LabX XRD-6100 X-ray diffractometer with Cu Kα radiation (40 kV, 30 mA) of wavelength 0.15418 nm (SHIMADZU, Japan). SEM measurements were performed on a XL30 ESEM FEG scanning electron microscope at an accelerating voltage of 20 kV. TEM measurements were performed on a HITACHI H-8100 electron microscopy (Hitachi, Tokyo, Japan) with an accelerating voltage of 200 kV.

Preparation of P-AgBr and BD-Ag: Typically, P-AgBr was prepared by an anodic oxidation method using a RPS3003C-2 adjustable DC regulated power supply (SHENZHEN MEIRUIKE TECHNOLOGY CO.). The Ag foil was cleaned by immersion and sonication for 15 min sequentially in acetone, ethanol, and then deionized water. The cleaned Ag foil mesh (2 cm × 2 cm) was anodized in the electrolyte containing 39 mL ethylene glycol, 1 mL of 0.5 wt% NaBr aqueous solution with a platinum foil as a counter electrode at 32 V for 30 min. The BD-Ag was synthetized by reducing the as-prepared P-AgBr in 0.5 M CO_2-saturated preelectrolyzed $KHCO_3$ solution at –1.2 V (vs. Ag/AgCl, 3 M KCl) for 2 h. After the reduction process, the electrochemical cell was thoroughly rinsed and filled with fresh 0.5 M pre-electrolyzed $KHCO_3$ solution and purged with CO_2 to perform the CO_2 reduction reaction. In order to further confirm the influence of surface Br^- on the CO_2 reduction activity, the BD-Ag sample was annealed in a H_2 atmosphere at 400 °C for 2 h to remove the adsorbed Br^- from the Ag surface while retaining the porous nanowire structure.

Electrochemical measurements and product analyses: Electrochemical

measurements were performed with a CHI 660E electrochemical analyzer (CH Instruments, Inc., Shanghai) in a customized H-type cell separated by a Nafion ® 115 membrane with 0.5 M $KHCO_3$. A standard three-electrode system used a BD-Ag/Ag foil (0.5 cm × 0.5 cm) as the working electrode. A graphite rod and an Ag/AgCl were used as the counter electrode and the reference electrode, respectively. The potentials reported in this work were calibrated to RHE, using the following equation: E (RHE) = E (Ag/AgCl) + (0.197 + 0.059 pH) V. All the potentials were reported versus RHE unless otherwise noted. Polarization curves were obtained using linear sweep voltammetry with a scan rate of 10 mV s^{-1}. The temperature of the solution was maintained at around 25 °C during the whole measurements process. The as-generated gas was carried into a gas chromatograph (SC-3000B online system) every 20 min during CO_2 electrolysis for detection of products. A representative set of GC data obtained during CO_2 electroreduction on BD-Ag is presented in Table S1.

Table S1. Data obtained from the GC analysis of CO_2 reduction products using BD-Ag at −0.6V. The volume of the sampling loops are 1 cm^3

Sample	Time of sample injection (s)	Current (mA)	Volume concentration of CO (ppm)
1	3000	2.982	544.90
2	4200	2.981	545.28
3	5400	2.982	545.52
4	6600	2.984	546.34
5	7800	2.983	545.88
6	9000	2.982	545.58
Average		2.982	545.58

The Faradaic efficiency (FE) of CO was calculated as below:[1]

$$FE = \frac{2Fv_jGP}{RTi_{total}} \times 100\%$$

Where v_j (vol%) is the volume concentration of CO in the exhaust gas from the electrochemical cell (GC date), G is Gas flow rate, i_{total} (A) is the steady-state cell

current, P=1.01×10^5 Pa, T=273.15 K, F=96485 C mol^{-1}, R=8.314 J $mol\ K^{-1}$.

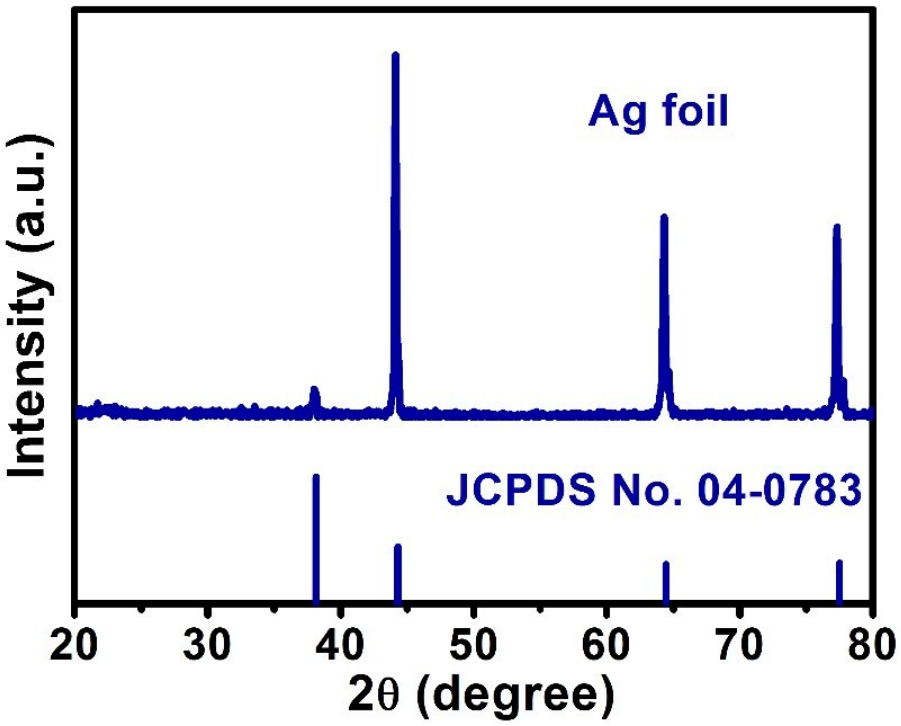

Fig. S1. XRD pattern of blank Ag foil.

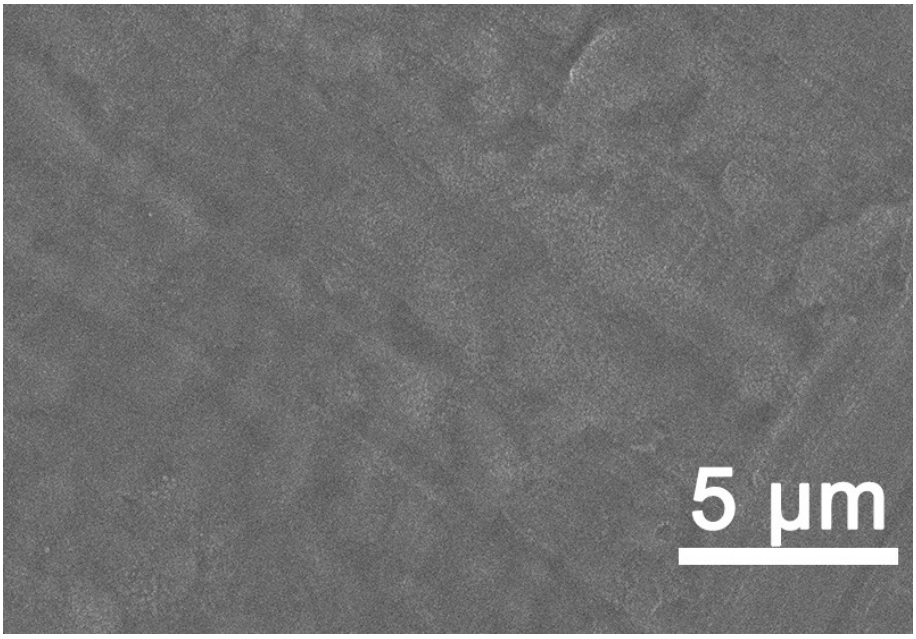

Fig. S2. SEM image of blank Ag foil.

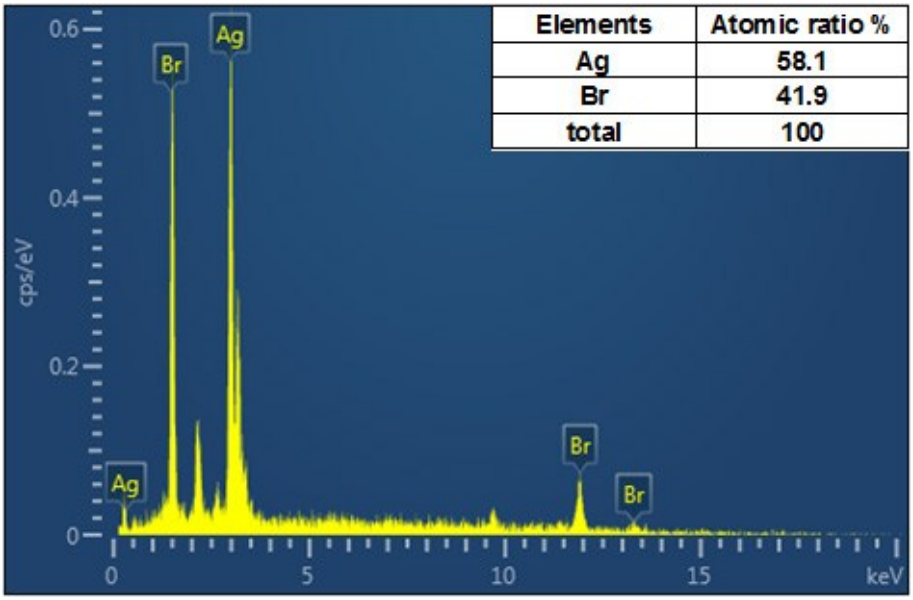

Fig. S3. EDX spectrum of P-AgBr.

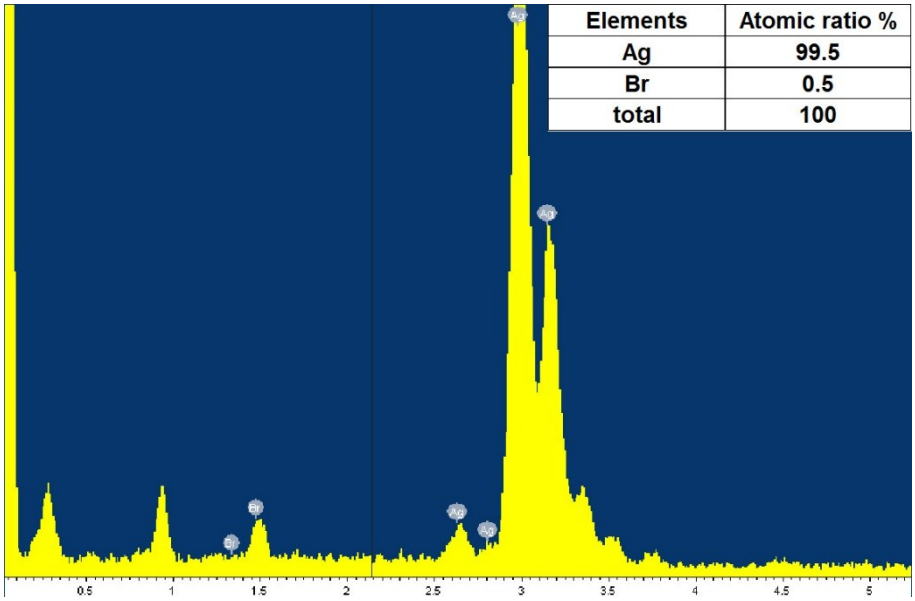

Fig. S4. EDX spectrum of BD-Ag.

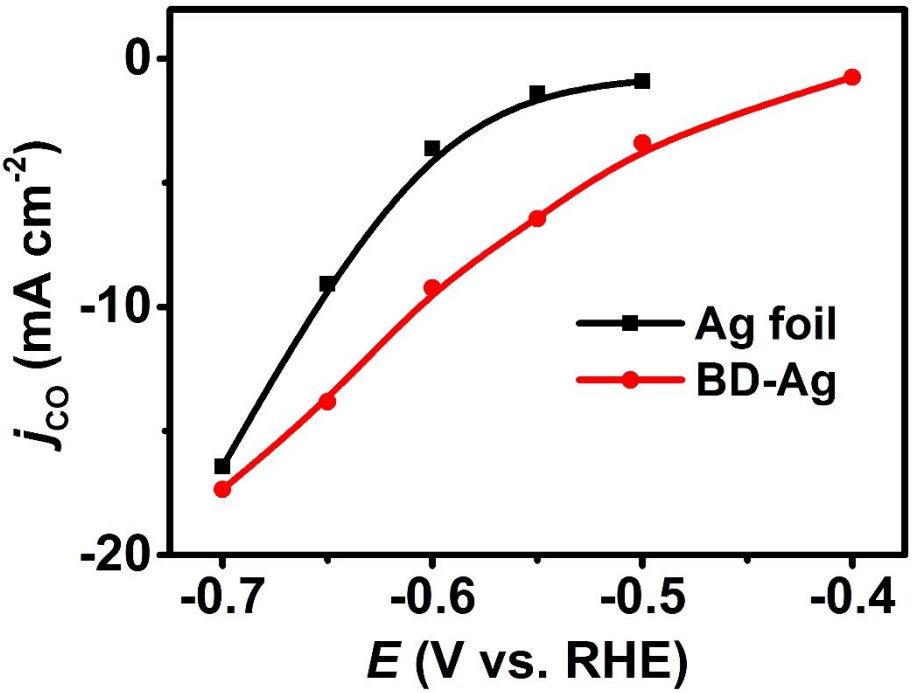

Fig. S5. The CO partial current densities at various potentials normalized by electrochemical surface area.

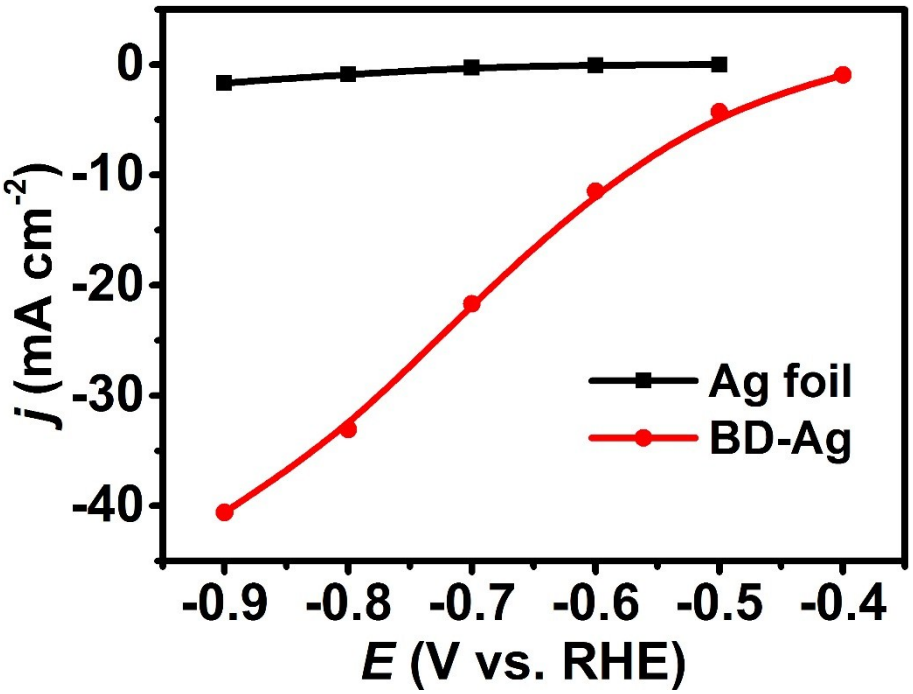

Fig. S6. Current densities for CO at various potentials.

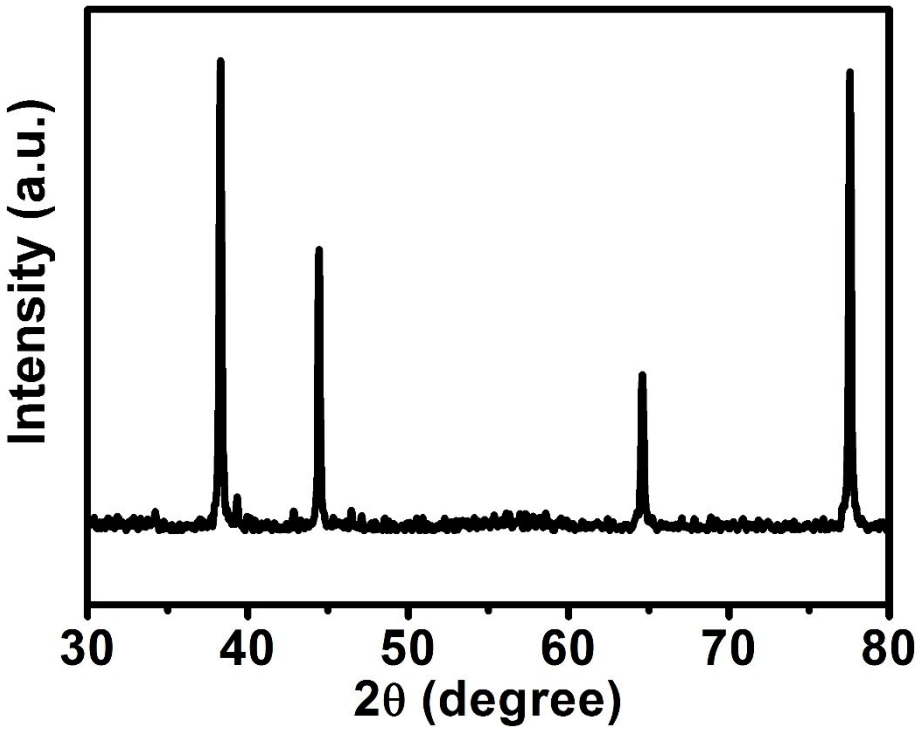

Fig. S7. XRD pattern for BD-Ag after stability test.

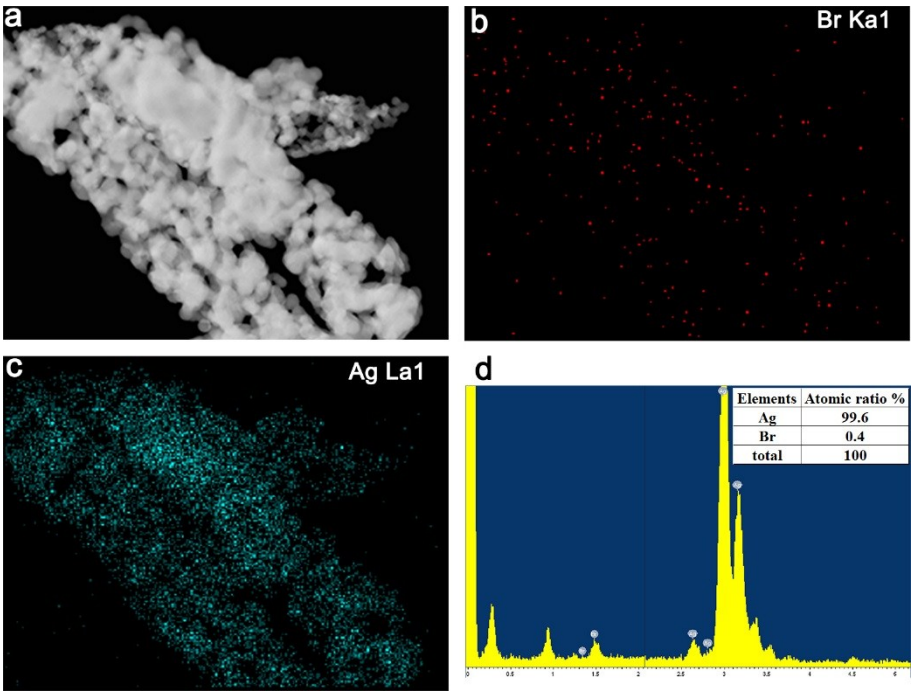

Fig. S8. (a) STEM image, EDX elemental mapping images of (b) Br and (c) Ag, and (d) EDX spectrum for BD-Ag after stability test.

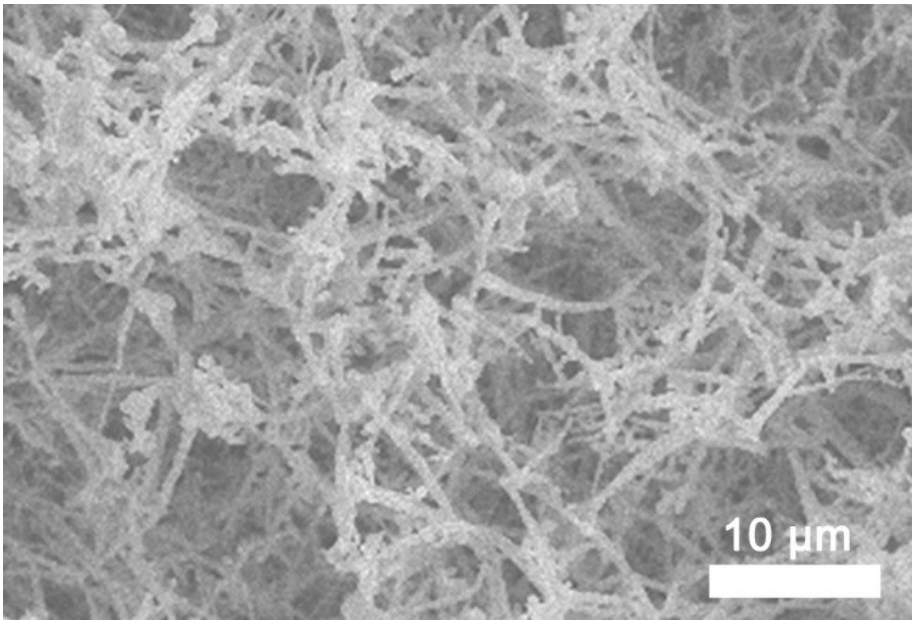

Fig. S9. SEM image for BD-Ag after H_2 annealing.

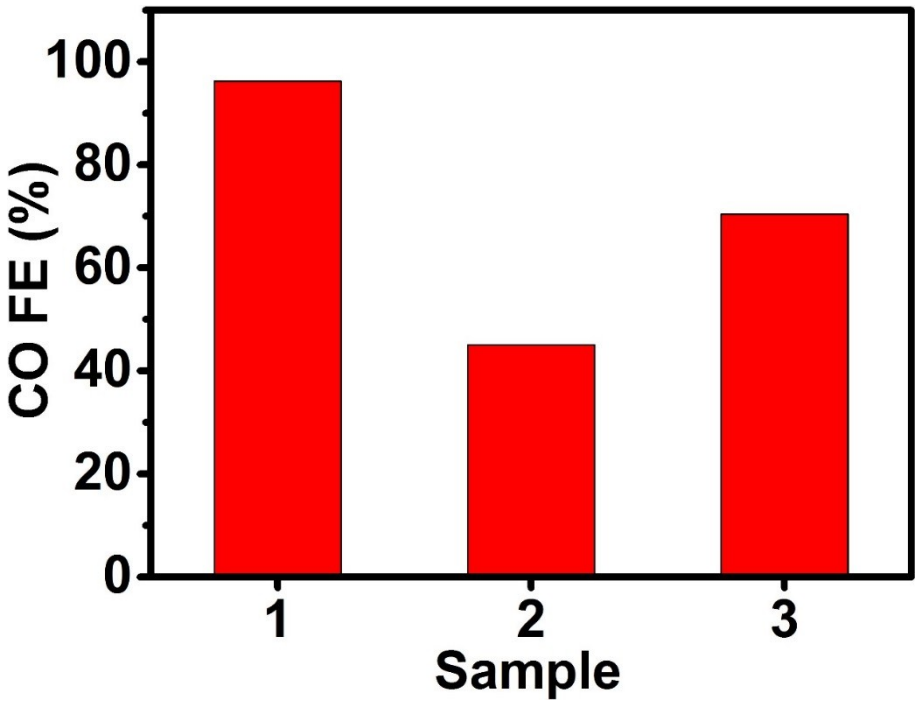

Fig. S10. FE of CO on BD-Ag before (sample 1) and after (sample 2) H_2 annealing in CO_2-saturated 0.5 M $KHCO_3$, BD-Ag after H_2 annealing in CO_2-saturated 0.45 M $KHCO_3$ + 0.05 M KBr (sample 3) at –0.6 V.

Table S2. The comparison of FE for CO_2 electroreduction to CO with other reported Ag-based electrocatalysts.

Catalyst	Potential	j_{CO}[a] (mA cm^{-2})	Electrolyte	FE (%)	Ref.
BD-Ag	−0.6 V	11.50	0.5 M $KHCO_3$	96.2	This work
mesostructured silver inverse opal	−0.7 V	About 15	0.1 M $KHCO_3$	80	2
Ag foil	−1.72 V vs. Pt wire	~6 (total current densities)	1-butyl-3-methyl-imidazolium trifluoromethane sulfonates in propylene carbonate	63.3	3
Ag nanoparticles 3 nm 5nm 10nm	−0.75 V	~7.5 (−0.9V) ~8 (−0.75V) ~3 (−0.95V)	0.5 M $KHCO_3$	76.8 88.4 70.5	4
nanoporous silver Ag	−0.5 V	~9	0.5 M $KHCO_3$	90	5
Bulk Ag	−1.5 V	−	EMIM-BF_4 in water	96	6
coral-like Ag	−0.6 V	6.62	0.1 M $KHCO_3$	95	7
triangular silver nanoplates	−0.855 V	~1.25	0.1 M $KHCO_3$	96.8	8
oxide-derived nanostructured Ag	−0.8 V	1	0.1 M $KHCO_3$	89	9

plasma-treated Ag foils	−0.6 V	~2.1	0.1 M $KHCO_3$	90	10
ID-Ag	−0.7 V	16.7 (total)	0.5 M $KHCO_3$	94.5	11

[a] CO partial current density under the overpotential noted in the left column unless the bias potential is noted

References

1 W. Zhu, R. Michalsky, Ö. Metin, H. Lv, S. Guo, C. J. Wright, X. Sun, A. A. Peterson and S. Sun, *J. Am. Chem. Soc.*, 2013, **135**, 16833−16836.

2 Y. Yoon, A. S. Hall and Y. Surendranath, *Angew. Chem.*, *Int. Ed.*, 2016, **55**, 15282−15286.

3 J. Shi, F. Shi, N. Song, J.-X. Liu, X.-K. Yang, Y.-J. Jia, Z.-W. Xiao and P. Du, *J. Power Sources*, 2014, **259**, 50−53.

4 C. Kim, H. S. Jeon, T. Eom, M. S. Jee, H. Kim, C. M. Friend, B. K. Min and Y. J. Hwang, *J. Am. Chem. Soc.*, 2015, **137**, 13844–13850.

5 Q. Lu, J. Rosen, Y. Zhou, G. S. Hutchings, Y. C. Kimmel, J. G. Chen and F. Jiao, *Nat. Commun.*, 2014, **5**, 3242.

6 B. A. Rosen, A. Salehi-Khojin, M. R. Thorson, W. Zhu, D. T. Whipple, P. J. A. Kenis and R. I. Masel, *Science*, 2011, **334**, 643–644.

7 Y.-C. Hsieh, S. D. Senanayake, Y. Zhang, W. Xu and D. E. Polyansky, *ACS Catal.*, 2015, **5**, 5349–5356.

8 S. Liu, H. Tao, L. Zeng, Q. Liu, Z. Xu, Q. Liu and J. L. Luo, *J. Am. Chem. Soc.*, 2017, **139**, 2160–2163.

9 M. Ma, B. J. Trześniewski, J. Xie and W. A. Smith, *Angew. Chem.*, *Int. Ed.*, 2016, **55**, 9748–9752.

10 H. Mistry, Y.-W. Choi, A. Bagger, F. Scholten, C. S. Bonifacio, I. Sinev, N. J. Divins, I. Zegkinoglou, H. S. Jeon, K. Kisslinger, E. A. Stach, J. C. Yang, J. Rossmeisl and B. R. Cuenya, *Angew. Chem.*, *Int. Ed.*, 2017, **56**, 11394–11398.

11 Y. Zhang, L. Ji, W. Qiu, X. Shi, A. M. Asiri and X. Sun, *Chem. Commun.,* 2018, **54**, 2666–2669